



## Synthesis and structural characterization of $\text{La}_{.5}\text{Ca}_{.25}\text{Sr}_{.25}\text{MnO}_3$

M. C. Kornfield,<sup>✦</sup> Mentors: Dr. S. Wicker<sup>‡</sup> and Dr. L. L. Henry<sup>‡</sup>

<sup>✦</sup>Participant in LA-SiGMA summer REU program at Southern University, Undergraduate at Georgetown University <sup>‡</sup>Department of Chemistry, Southern University <sup>‡</sup>Department of Physics, Southern University

---

### Abstract:

*This paper covers two separate methods of synthesis: solid-state and solution based, which we utilized in order to create a difference in particle size. The solid-state method produced microcrystals while the solution-based method produced nanoparticles. Both sets of products and reactants were studied with X-Ray Diffraction, a Scanning Electron Microscope, and Thermogravimetric Analysis/Differential Scanning Calorimetry. These analysis tools were used to formulate the crystal structure of the material, as well as refine and verify the results of the synthesis process. The material was found to have a perovskite structure with space group  $Pbnm$ , and we verified the creation of nanoparticles.*

---

### 1. Introduction

The class of ceramic-based perovskites that exhibit Colossal Magnetoresistance is a source of great interest to the field of “spintronics,” an electrical engineering application that utilizes the spin of electrons to regulate electric circuits.<sup>1</sup> These ceramic-perovskites are made of a rare earth metal (La, Eu, Gd) doped with an alkaline earth metal (Sr, Ca, Ba), which is then combined with a magnetic oxide ( $\text{MnO}_3$ ,  $\text{FeO}_3$ ). Possible applications have been noted about this class of materials, based on paramagnetic, ferromagnetic, and antiferromagnetic transitions of the material at different temperatures.<sup>2,3</sup> One of the general trends in papers on the topic of these materials is that the doping percentage is generally quite low and only one alkaline earth metal is used for doping.

Our project sought to synthesize and do preliminary studies on a material that was outside the generic CMR-exhibiting perovskites. Our desired product was

$\text{La}_{.5}\text{Sr}_{.25}\text{Ca}_{.25}\text{MnO}_3$ , or Lanthanum Strontium Calcium Manganate (LSCMO). A previous REU student had synthesized this material; unfortunately the attempt to produce nanoparticles was unsuccessful. This paper will present a different synthesis route that produced the desired nanostructured material. Rigorous documentation of the solid-state synthesis process (done for comparison’s sake) that we used as well as documentation for the newly developed process of producing nanoparticles is presented. The production of nanoparticles required a literature review of various wet chemical methods that are similar to the method we utilized.<sup>4,5,6,7</sup> The main reason a solution method is required is that heating at high temperatures calcifies the material, preventing the production of nanoparticles, and we wanted to avoid the stress induced by mechano-chemical processing (we also lacked necessary nanopowders). We utilized many different instruments to refine the synthesis process; the analysis and a brief description of the results are included in the report. In addition, we

determined the crystal structure of our material based off of the XRD data that we collected and analyzed, and based off of the comparisons made with previous information on the structure of perovskites.

## 2. Experimental

### Methods

The solid-state heating procedures were performed using furnaces at temperatures up to 1500°C. Sol-gel heating was performed at lower temperatures, in a vented oven and a furnace under 100% oxygen partial pressure.

For our compositions determination, a JEOL JSM-6340 Scanning Electron Microscope (SEM) identified particle size and distribution via Electron-Dispersive X-ray Spectroscopy (EDAX), a TA® SDT performed Thermogravimetric Analysis and Differential Scanning Calorimetry (TGA/DSC) under 40mL/min air flow, while a TA® Q10 performed a more sensitive DSC measurement, and an XRD (X-ray Diffraction) Diffractometer with a Bruker® copper anode tube XRD (at 40kV and 40mA) scanned from  $10^{\circ}\text{C} < 2\theta < 120^{\circ}$  to identify phases and crystal structure. Analysis of the XRD data included structural refinement techniques performed on GSAS and Topaz. We performed structural modeling of the crystal by using Crystal Maker® software.

### Procedure

**I.** For our solid-state synthesis, we mixed together our stoichiometric amounts of high purity (99.999 %) starting powders (lanthanum oxide, strontium carbonate, calcium carbonate, and manganese oxide) together with a binder solution (B98, a low temperature melting point organic compound). We pressed ten 25 mm pellets, each weighing approximately 1.3 grams and heated them at different temperatures. The temperatures varied, with

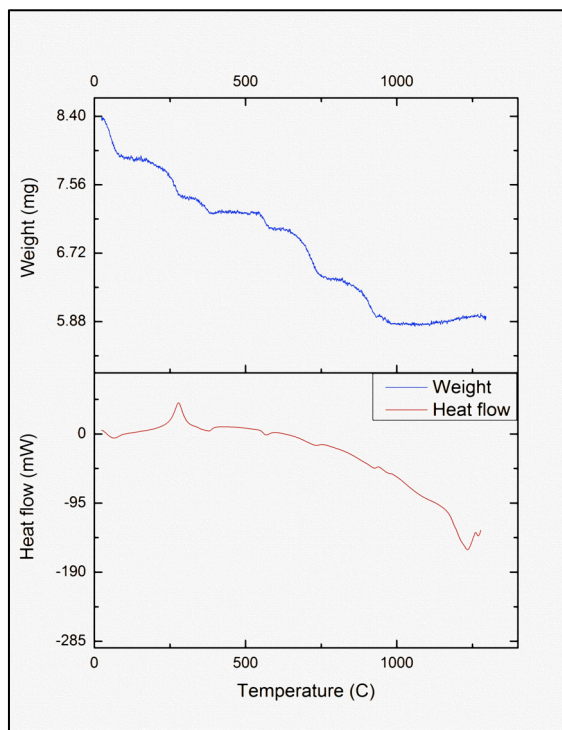


**Figure 1: TGA/DSC, with temperature against weight and heat flow, demonstrates phase purity by 1000°C. Notice the exothermic spike at 250°C shows the burning of binder, and the weight gain at 1250°C demonstrates the binding of oxygen.**

max heating values at 1000°C, 1250°C and 1500°C. The samples were subjected to TGA/DSC investigation to determine optimal heating temperatures. Examination of the data showed the materials were all melted by 1000°C (Figure 1). However, as we will later see, we needed to calcify the materials, so we used heat treatments at higher temperatures after the initial firings. We did this to close up the void spaces and to improve the distribution of each element in the material.

**II.** For our solution-based method, we formed a precursor solution. Since we did not have all the nitrates we needed (we only had manganese nitrate) we first dissolved the three powders (lanthanum hydroxide, strontium hydroxide, and calcium carbonate) in nitric acid to form the nitrates, then we added manganese nitrate and oxalic acid, oxalic acid being the coordinating compound used to form the precursor solution. Once all the materials were dissolved, we adjusted the pH from 1 to 10 with ammonium hydroxide to cause the

material to precipitate, and then evaporated the excess solution to form a gel. We next heated the gel at 600°C for 12 hours to burn the precursor away and create the nanoparticles. We verified the existence of nanoparticles through the use of an SEM and a qualitative analysis of the XRD. To reduce the undesired phases that were present, we fired the nanoparticles at 900°C for 8 hours under 100% oxygen partial pressure to force the required reaction to go forward.

### 3. Results and Discussion

The TGA/DSC measurement shown below is of the phase pure LSCMO and it can be seen that the weight loss amounts are very small (scale in milligrams). But the major spike in heat flow and weight gain at the end of the run (performed at a rate of 20°C/min) demonstrates

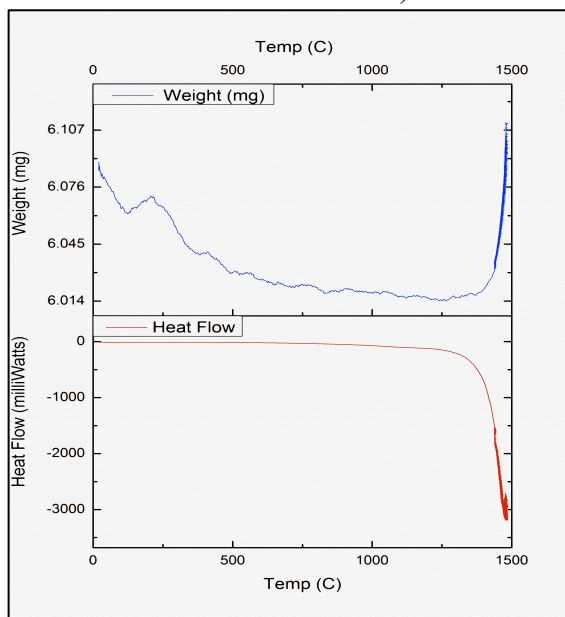


Figure 2: TGA/DSC of the phase pure material, demonstrating rapid oxidization, shows temperatures compared against heat flow and weight

an enormous heat change, on the order of 3 watts. We believe this spike is due to the rapid addition of oxygen to the system, shown in the previous TGA/DSC, as there may be oxygen defects within the crystal structure. These defects may then be filled by oxygen in the air that is drawn into the excited crystal lattice, producing a large endothermic spike.

The SEM analysis was not limited to just the pictures from which we gained a qualitative measurement of the size of the particles, but it also included a quantitative measurement of the concentration of the material, via the EDAX detector. We can see on the two pictures below taken from the SEM the size difference between the two materials from different synthesis routes. The scale is slightly different, but the thing to note is the flowering in the top picture shows that the material is an aggregate of smaller particles, while the clearly defined shapes of

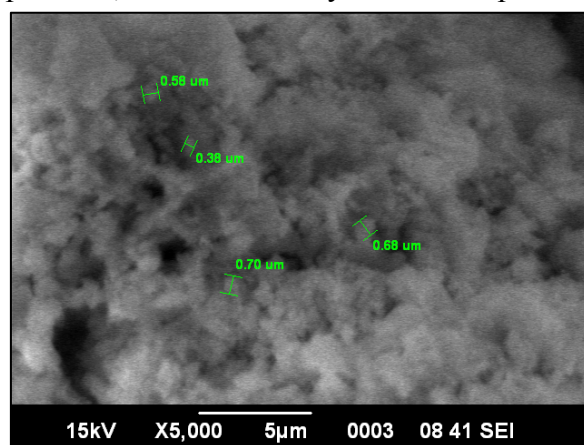
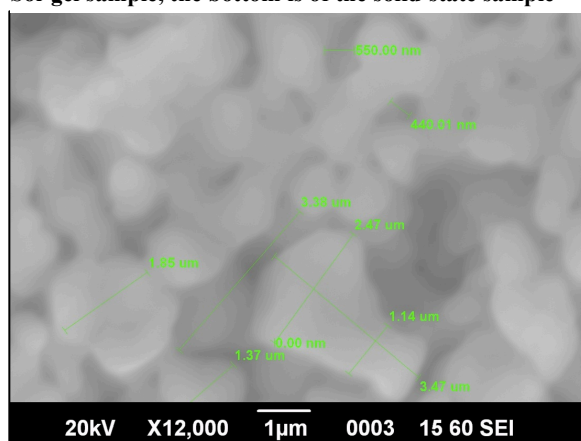


Figure 3: SEM of LSCMO particles, the top is of the Sol-gel sample, the bottom is of the solid-state sample



the lower picture demonstrate solid microcrystals. Some issues arose when collecting data with the SEM, due to charge buildup on the insulating particles. This made resolution at higher magnifications almost impossible, and prevented a more accurate depiction of the nanoparticles. Still, with the presented pictures, we can infer particle size, as

well as by analyzing the XRD of the products of the solution based method.

Below we have the EDAX reading, which was done on the LSCMO produced by the solid-state reaction synthesis route. There is the slight presence of carbon but otherwise all of the diffraction intensity peaks that verified the desired composition were present. Other peaks present on the graph represent the penetration of the electrons through multiple layers of the electron shells (penetration of k-edge, l-edge, etc.) We also have a figure showing the improvement of calcium distribution (also captured via EDAX) and that demonstrates how the higher firing temperatures helped to smooth out the distribution of our material.

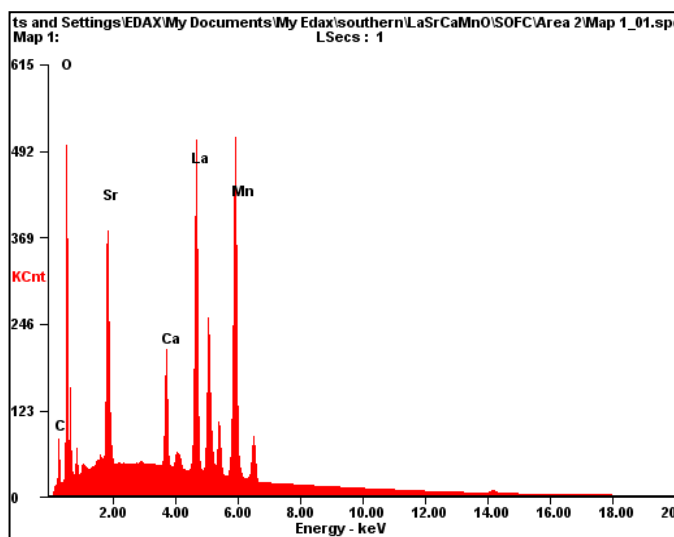


Figure 4: EDAX of solid-state LSCMO, where x is the energy emitted in eV and y is the intensity detected, shows small concentration of carbon but the presence of the other desired materials as well

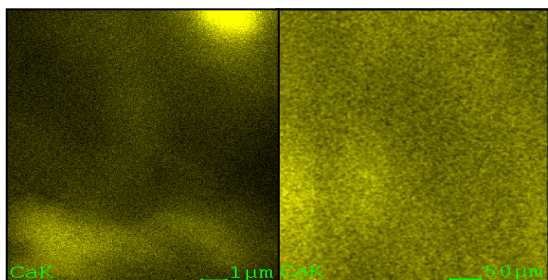


Figure 5: EDAX distribution identification, showing on the left is the LSCMO fired at 1000°C compared with the right side, which is the material fired at 1200°C

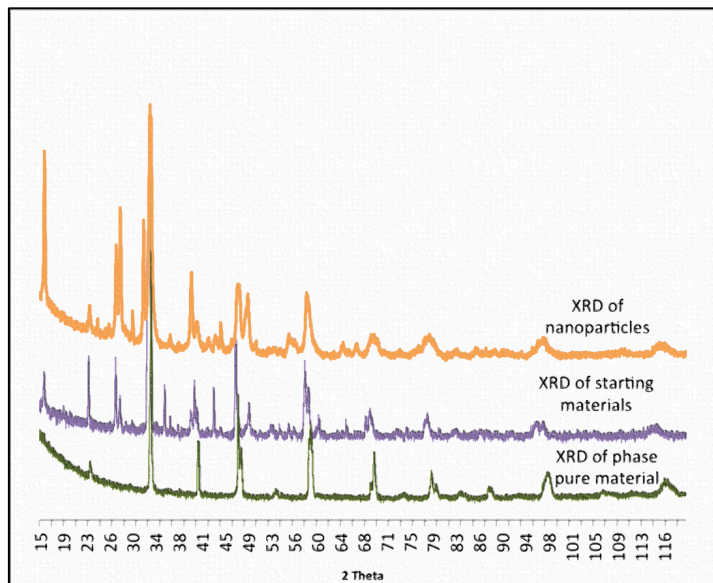


Figure 6: XRD from  $2\theta = 15^\circ$  to  $120^\circ$  compared against intensity, Top shows sol-gel method, middle shows unreacted material, bottom shows material after firing at  $1500^\circ\text{C}$

The XRD data demonstrated a phase pure material when fired at  $1500^\circ\text{C}$ . We can view the phase purity qualitatively, by seeing the existence of a small number of peaks, resulting from the GSAS refinements discussed below. On top we see the XRD of supposed nanoparticles, whose size we can guess is quite small, based on the large full-width half max increase from the starting material, since FWHM is inversely related to the size of a particle in X-ray Diffraction. The pattern of peaks in the solid-state prepared sample's XRD shows a high symmetry pattern. This is supported by the literature, which indicates the crystal structure is cubic perovskite.<sup>8</sup>

Speaking of the crystal structure, we were able to determine the shape of this compound using analysis tools such as GSAS and Topaz to refine some CIFs (crystallographic information files) and then put these CIFs into Crystal Maker® to form a 3D model of our material. The next page will demonstrate the different pieces that went into this crystal analysis: the graph comparing the calculated and observed values of the phase pure material (Figure 7), the CIF file window shown in GSAS (Tables 1 and 2), and their product, the 3D model (Figure 8),

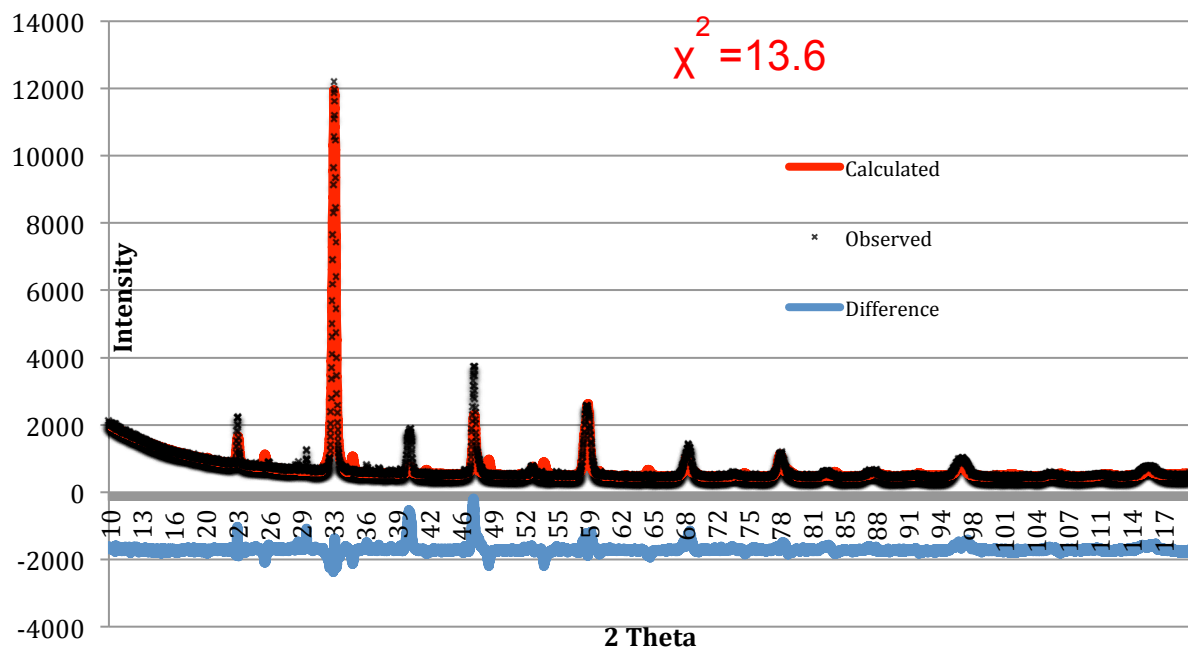


Figure 7: XRD shown up above, with a CIF file developed on GSAS as the calculated value, plotted with the observed value and the difference between the two,

Name	Fractional x-coordinates	Fractional y-coordinates	Fractional z-coordinates	Multiplicity	Occupancy	U <sub>iso</sub>
Mn1	½	0	0	4	1	0.025
O1	0.043690	1.682300	¼	4	1	0.8
O2	2.128730	0.492400	-0.41549	8	1	0.8
La1	-0.00630	0.044300	¼	4	0.5	0.025
Sr1	-0.00630	0.044300	¼	4	0.25	0.025
Ca1	-0.00630	0.044300	¼	4	0.25	0.025

Table 1: Shows certain values from the CIF file, which demonstrate atomic position and thermal parameters for the materials in the unit cell. The fractional coordinates are translated using Wycoff positions to develop a full crystal

Space group:	Lau Class:	
Pbnm	mmm	
a : 5.416	b : 5.416	c 7.646
α : 90.0	β : 90.0	γ 90.0

Table 2: Other important information from the CIF file, which gives the length of the cell in each direction, as well as the associated angles, and the space group, which tells us about the symmetry locations

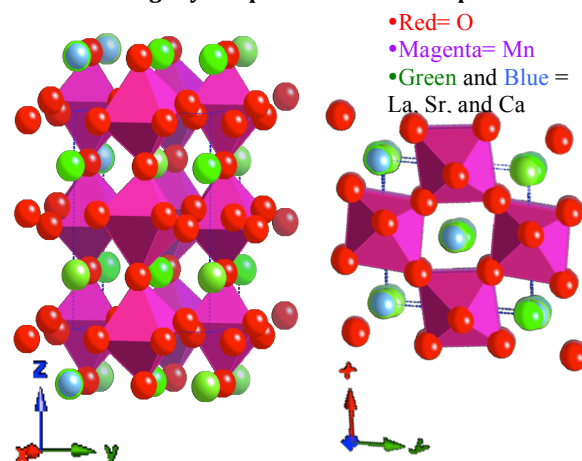


Figure 8: Image created on Crystal Maker using the CIF file

all of which will be of great importance when we perform the necessary magnetic measurements on the material, and want to try and ascribe certain effects to a structural element.

We obtained the Wyckoff positions and the space group (specific crystallographic details) to complete our CIFs from the literature<sup>8</sup>, and came up with all of the other values by manipulating the variables in the GSAS procedure and refining certain values to try and lower the  $\chi^2$  value (a statistical value that shows higher correlation as it gets smaller). The final  $\chi^2$  that this CIF file created was about 13.6, something that suggests a strong correlation between the calculated plot and the observed plot. The one exception was one peak that did not seem to fit (notice back in Figure 6 the 3rd peak has no calculated fit). We used GSAS to also identify the purity of the sample, which was identified as 96% pure.

One issue that will require further research was the fact that multiple space groups fit our data for the crystallographic information, as in R-3c from one source<sup>9</sup> and Pbnm from another.<sup>8</sup> Both gave very small values of  $\chi^2$  but the R-3c presented difficulties when it came to the placement into crystal maker. Further crystallographic studies will need to be performed to determine the best fit.

The SEM showed only inferable evidence for the existence of nanoparticles, so it is by no means a conclusive piece of evidence. If it were possible, a TEM would have been much preferable to verify the existence of nanoparticles in the LSCMO sample prepared via the wet chemical method. One important piece of data that supports the inferences drawn from the SEM is the aforementioned XRD that demonstrates the increase in the full-width half max of the material once fired in the sol-gel method. Our EDAX report verified that the proper elements were present in the

material, and the error values associated with the weight percentages were considered too unreasonable to trust as a source of true stoichiometric evaluation.

In any case, only doubt remains as to whether or not we have the true stoichiometric ratio, and further research will be required to verify this information. Possibilities include the use of AAS (atomic absorption spectrum) and XRF (X-ray fluorescence) to find the true stoichiometry.

Our work relates back well to the literature, since our synthesis method involved mixing a coordinating compound in with solution forms of the materials to form a precursor solution.<sup>6,10</sup> A comparison of full width half max was also performed in order to link the material to nanoparticles.<sup>7</sup> The main divergence from the literature is our lack of magnetic characterization, something that we were unable to perform with our limited time.

#### 4. Conclusion

Our findings presented here are simply the experimental verifications of our physical results, those physical results being the materials produced for this report. The nanoparticles and the solid-state materials were certainly not the end goal, but they are a necessary part of the process of performing these CMR measurements, and continuing the work of Dr. Henry.<sup>11</sup> By extending our study to the nano-scale, we are beginning a more diverse study of  $\text{La}_{.5}\text{Sr}_{.25}\text{Ca}_{.25}\text{MnO}_3$ 's magnetic properties.

Another accomplishment of this report was to perform structural analysis on the crystal lattice of this material, which had never been done before (for this specific doping arrangement). This may become very useful when trying to find a structural cause of the material's magnetic properties.

This work should only be viewed as a

preliminary endeavor. Not only do we need to measure the magnetic properties, but also we must refine the synthesis process further, using the aforementioned AAS and XRF for stoichiometry, but also to measure functional groups during the synthesis process, we can perform FTIR measurements and also we can create more samples to create a more valid future report.

This was only the beginning, hopefully a beginning that has brought us towards a more exhaustive analysis of LSCMO.

## References

1. Sebastian Anthony (2012). *Extreme Tech* [online]. Available from: <<http://www.extremetech.com/computing/131230-cpus-of-the-future-amd-partners-with-arm-while-intel-designs-a-brain-on-a-chip>>. [Accessed 7/19].
2. M. Muroi, P. G. McCormick and R. Street (2003, June). *Surface spin disorder and exchange bias in  $La_{0.7}Ca_{0.3}MnO_3$  nanoparticles synthesized by mechanochemical processing*. (Rev. Adv. Mater. Sci. 5). Advanced Nano Technologies and The University of Western Australia, Welshpool, Australia.
3. B. Roy, A. Poddar, and S. Das (2006, May). *Electrical transport properties and magnetic cluster glass behavior of  $Nd_{0.7}Sr_{0.3}MnO_3$  nanoparticles*. (Journal of Applied Physics 100). Saha Institute of Nuclear Physics, Kolkata, India.
4. Dong-Hwang Chen, Min-Hung Liao (2001, November). *Preparation and characterization of YADH-bound magnetic nanoparticles*. (Journal of Molecular Catalysis B: Enzymatic 16). Department of Chemical Engineering. National Cheng Kung University, Tainan, Taiwan.
5. Zhanhu Guo, Laurence L. Henry, Vadim Palshin and Elizabeth J. Podlaha (2005, December). *Synthesis of poly(methyl methacrylate) stabilized colloidal zero-valence metallic nanoparticles*. (J. Mater. Chem. 16). LSU and Southern University, Baton Rouge, Louisiana.
6. G. Wang, Z. -D. Wang, L. -D. Zhang (2005, May). *Preparation and magnetocaloric effect of  $(La_{0.67-x}Gdx)Sr_{0.33}MnO_3$  ( $X=0.1, 0.15$ ) nanoparticles*. (Appl. Phys. A 80). Institute of Solid State Physics, Chinese Academy of Sciences, Hefei, P. R. China.
7. R. Mahesh, R. Mahendiran, A. K. Raychaudhuri, and C. N. R. Rao (1996, February). *Effect of particle size on the giant magnetoresistance of  $La_{0.7}Ca_{0.3}MnO_3$* . (Appl. Phys Lett. 68). Indian Institute of Science, Bangalore, India.
8. I.S. Ahmed Farag, A. M Mostafa and I.A. Abdel-Latif (2007, ?). *Preparation and Structural Characterization of  $Eu_{0.65}Sr_{0.3}Mn_{1.0}Fe_xO_3$* . (Egypt. J. Solids, Vol. (30), No. (1)). Solid State Department, National Research Center, Dokki, Giza, Egypt.
9. P. Norby, I. G. Krogh Anderson, E. Krogh Andersen (2002, October). *The crystal structure of lanthanum manganate (iii),  $LaMnO_3$ , at room temperature and at 1273 K under  $N_2$* . (Journal of Solid State Chemistry 1). Department of Chemistry, University of Odense, Odense M, Denmark. Available from: <<http://www.sciencedirect.com/science/article/pii/S002245969580028N>>. Accessed: 7/24/12.
10. Yun-Hui Huang, Zhi-Gang Xu, Chun-Hua Yan, Zhe-Ming Wang, Tao Zhu, Chun-Sheng Liao, Song Gao, Guang-Xian Xu (2000, January). *Soft chemical synthesis and transport properties of  $La_{0.7}Sr_{0.3}MnO_3$  granular perovskites*. (Solid State Communications 114). Peking University, Beijing, China. Available from: <<http://www.chem.pku.edu.cn/mmm/publications/publications/solidstatecommun/huangyh00.pdf>>. Accessed: 7/19/12.
11. L. L. Henry and A. Harvey Jr. *Systematic investigation of magnetization, magnetoresistance, and heat capacity of polycrystalline  $La_{0.5}(Ca_{0.5-x}Sr_x)MnO_3$  for  $x=0.0, 0.1, 0.25, 0.4, 0.5$  in the 5k to 300K Temperature Range*. (Unpublished). Southern University, Baton Rouge, Louisiana.

## Acknowledgements

"This material is based upon work supported by the National Science Foundation under the NSF EPSCoR Cooperative Agreement No. EPS-1003897 with additional support from the Louisiana Board of Regents."